

Spatially Resolved Online Leak Detection in a Baghouse Filter Applying Low-Cost PM-Sensors

Peter Bächler*, Jörg Meyer, and Achim Dittler

DOI: 10.1002/cite.202200116

 This is an open access article under the terms of the Creative Commons Attribution License, which permits use, distribution and reproduction in any medium, provided the original work is properly cited.



Supporting Information
available online

Dedicated to Prof. Dr.-Ing. Joachim Werther on the occasion of his 80th birthday

Conventional particle emission measurement technology only takes into account the total emission and does not offer spatial resolution. Extensive troubleshooting is required in order to identify potential emission hotspots (e.g., small leaks) that contribute strongly to dust emissions. A network of inexpensive low-cost PM-sensors was used in a small-scale baghouse filter for spatial online particle emission monitoring. Different types of emission hotspots were investigated. Spatial PM monitoring enabled the reliable identification of the position of the hotspot as well as estimation of leak size.

Keywords: Baghouse filter, Emission monitoring, Filtration, Leak detection, Low-cost PM-sensor

Received: June 27, 2022; *revised:* October 04, 2022; *accepted:* November 10, 2022


1 Introduction

Modern filter media applied for particle separation in industrial pulse-jet cleaned filters (baghouse filters) can provide very low particle emission levels and enable sufficient protection of the environment and downstream unit operations from dust emissions [1]. During filter operation, dust is separated at the surface of the filter medium what leads to the formation of a dust cake with high separation efficiency. The dust cake is periodically removed (e.g., via jet pulse) in order to lower the differential pressure between raw-gas side and clean gas side to grant economic long-term operation [2,3]. After jet-pulse cleaning, a particle emission peak can be detected on the clean gas side (or locally at the corresponding filter element), as particles can briefly penetrate the unprotected previously regenerated filter medium [4]. Penetration mechanisms through filter media other than direct penetration (e.g., seepage) have also been proposed in the past [5] but play a subsidiary role. Dependent on the age and the surface properties of the filter medium as well as the raw gas-concentration and other operating parameters, the particle emission peak only occurs over several minutes or even seconds and rapidly decreases to a zero level [6]. Baghouse filters remain one of the state-of-the-art methods for industrial dust removal, but the operation and maintenance of the filters is not without individual challenges depending on process parameters, type of dust and gas composition [7].

Problems regarding stable filter operation occur, if the cycle time between individual cleaning events approaches

zero (Δp -controlled operation) or the differential pressure vastly exceeds the desired operation window (Δt -controlled operation) [8,9]. These effects can be caused by an increase of residual pressure drop over the course of long-term filter operation. Especially nanoparticles can lead to clogging and significant aging of the filter medium, so that e.g., filtration of a pre-coat consisting of coarser particles may be necessary [10–12].

In the industrial application, the ideal emission behavior (emission peak after filter regeneration only) is seldom the case. Here, leaks of the filter bag (e.g., due to mechanical stress on the bag after many years of operation, pinhole leaks caused by sparks, abrasive dusts, particle penetration through the seams etc.) or the plenum plate (incorrectly installed filter elements, missing or damaged screws, etc.) can greatly contribute to the over-all dust emission [13–15]. Bach and Schmidt [16] investigated the contribution of small pinhole leaks in a filter test rig and Kurtz et al. [17] investigated the contribution of leaks in a small-scale baghouse filter. Both studies showed the dominating role of even small leaks (several ppm of installed filter area) on the total dust emission. Exceeding emission limits is one of the main reasons for shutdown of the plant or individual filter

Peter Bächler  <https://orcid.org/0000-0001-9172-5880>, Dr.-Ing. Jörg Meyer, Prof. Dr.-Ing. habil. Achim Dittler (peter.baechler@kit.edu)

Institute of Mechanical Process Engineering and Mechanics, Straße am Forum 8, 76137 Karlsruhe, Germany.

houses. The reliable detection of leaks is one of the most important challenges of the filtration industry [18].

Conventional monitoring systems for dust emissions are, e.g., gravimetric measurement or triboelectric sensors [19]. Gravimetric measurement requires averaging intervals in order to determine the total mass-based dust emission, offering no online information on the current emission. Triboelectric sensors offer a temporally resolved emission signal for the total dust emission on the clean gas side. However, even if a high continuous emission, hinting at a leak, is detected the origin of the emission hotspot remains unknown. In order to identify the position of a leak, a common method is the application of fluorescent dust, so that regions of increased particle penetration may be visually identified during a plant shutdown.

A cost-efficient and spatially applicable online monitoring tool could greatly help plant operators to identify local emission hotspots within the filter house. Li et al. employed an optical sensor, which could reliably detect a highly damaged filter bag (several cm² leak area) [20]. As previously stated, the range of potential damage on a filter bag is wide, as even small defects can cause a high emission contribution.

In previous studies, the potential of cheap, scattered-light-based low-cost PM-sensors has been investigated regarding their ability to correctly monitor the emission behavior of pulse-jet cleaned filters [6, 21, 22]. The sensors could reliably detect the PM-emission peak at the corresponding, previously regenerated, filter bag and showed qualitative agreement with a highly developed laboratory optical particle counter. Different (spatial) emission levels based on different filter media were investigated in a filter test rig and in a small-scale baghouse filter.

In this study, the suitability of the identification and localization of particle emission hotspots via low-cost PM-sensors is performed in a small-scale baghouse filter. On the one hand, spatial identification of a filter bag with open seams (whereby the seams enable high particle penetration during the initial filtration cycles) is investigated. Additionally, the impact of an increasing number of small leaks of several mm in diameter in a single filter bag on the measurement and detection capabilities of low-cost PM-sensors is shown.

2 Material and Methods

2.1 Objective of the Investigations

Previous investigations regarding spatial particle emission monitoring for pulse-jet cleaned filters mainly dealt with the overall characterization of the (spatial) emission behavior and validating the suitability of the low-cost PM-sensors for filtration applications. The characteristic emission behavior and distinct particle emission levels based on particle penetration through different filter media were identified in a filter test rig under defined conditions [21]. Additional investigations were performed in a small-scale baghouse fil-

ter with 9 filter bags under more praxis-relevant operation conditions. Ideal emission behavior (detection of a particle emission peak after filter regeneration of the corresponding filter bag only) was correctly detected by spatially deployed low-cost PM-sensors for membrane filter bags with sealed seams (low emission level, no emission contribution of the seams, etc.) [22]. The emission behavior for regular bags is different especially during the initial filtration cycles and for higher tank pressures for filter regeneration, as particles can penetrate the seams of the filter medium [6]. Clogging of the seams causes a decrease in particle emission and spatial particle emission peaks are detected at the corresponding filter bag after jet-pulse cleaning. Different particle emission levels could also be distinguished in the small-scale baghouse filter due to the measurement with low-cost PM-sensors. The local and total qualitative emission behavior corresponded well to reference measurements employing a highly developed laboratory optical particle counter.

One of the most prominent potential applications for spatial particle emission monitoring is the detection and identification of emission hotspots, as leaks may contribute greatly to the dust emission of pulse-jet cleaned filters, even exceeding the emission contribution of all installed filter elements that are in sound conditions [17, 18]. The objective of the presented measurements was the local identification and evaluation of the emission contribution of spatial particle emission hotspots. Different application scenarios were investigated according to Fig. 1.

In the first measurement campaign (scenario 1), all filter bags were made from medium A and the seams of all but one factory-new filter bag were sealed applying a sealing paste. This creates an emission dynamic, whereby one filter bag with the regular non-sealed seams contributes greatly to the overall dust emission, as particles can easily penetrate the seams of the filter bag during the initial filtration cycles [6, 14]. After several cycles, the seams are (mostly) clogged and the emission behavior approaches ideal behavior (detection of particle emission peak after filter regeneration only). This case represents a moderate fluctuating temporal emission hotspot. The position of the corresponding bag with non-sealed seams was varied in order to investigate the potential of the sensors to localize the particle emission hotspot within the baghouse filter. A similar experiment was shown in a previous publication for one filter position only [22].

In the second measurement campaign (scenario 2), filter bags made from medium B were installed. After previous measurement campaigns, consisting of approx. 400 filtration cycles, the emission behavior was close to ideal operation due to filter aging and clogging of the seams. Afterwards, the central filter bag (bag number 5) was pierced with a hot cannula of 3 mm diameter, creating a small leak. After 30 Δt -controlled overall filtration cycles for each filter bag, an additional hole was added (repetition of procedure up to six small leaks; exception for the case of four holes, where two additional holes were added). This scenario enables the detection of a strong spatial emission hotspot.

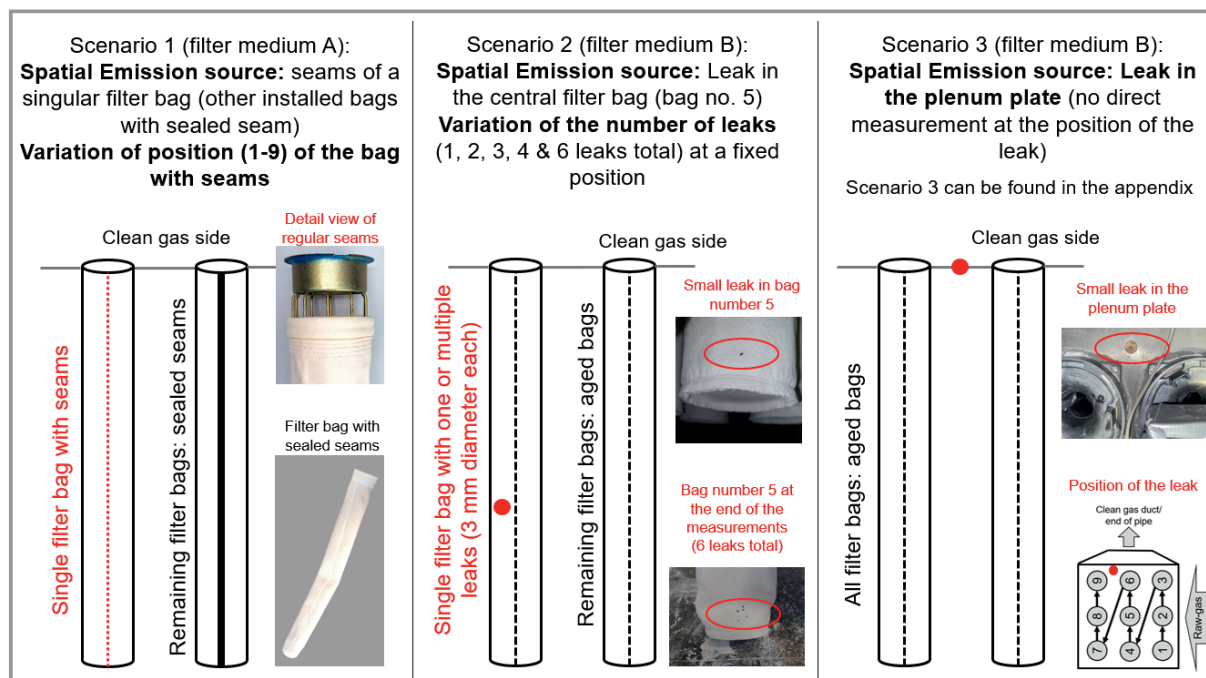


Figure 1. Overview of the different application scenarios for the detection of a spatial emission hotspot (scenario 3 in the appendix).

In addition to the implementation of leaks in the filter medium, a screw with a defined leak diameter of 4.2 mm was installed in the plenum plate without direct measurement in order to check, if a spatial emission hotspot further away from the sampling ducts of the spatially deployed low-cost PM-sensors could be identified (scenario 3, Supporting Information, SI).

2.2 Small-Scale Baghouse Filter

In Fig. 2, a schematic overview of the testing facility including the employed operating parameters is displayed. A radial blower creates a circulating air flow through the testing facility. Dust is dispersed into the raw gas at two separate points. Dust from a silo enables a steady supply of new dust and separated dust is recirculated back into the system in

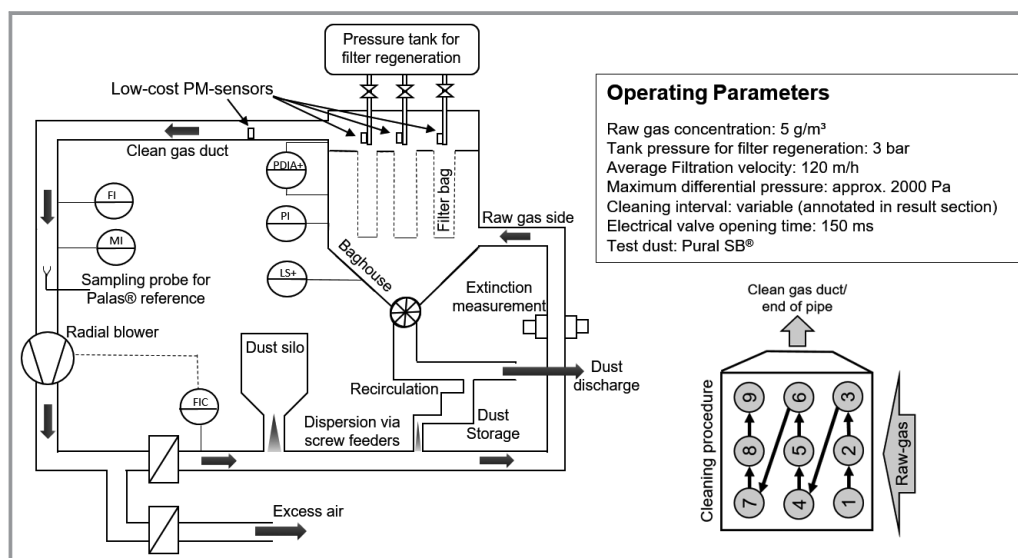


Figure 2. Schematic overview of the experimental facility including the small-scale baghouse filter (figure modified from [6, 22, 23]).

order to grant economic long-term operation. The raw-gas concentration is monitored at an extinction measurement, which has been calibrated to a mass-based raw-gas concentration of approx. 5 g m^{-3} .

The central element of the experimental facility is a small-scale baghouse with a total of nine filter bags (installed filter area of 4.14 m^2). The differential pressure between raw-gas side and clean-gas side is monitored and each filter bag can be regenerated individually by a jet pulse from the clean-gas side. During regeneration, the dust cake is detached from the filter surface and drops into the hopper. The employed cleaning strategy was a bag-by-bag cleaning algorithm. The cycle time between the individual filter regenerations varies between experiments and was kept above 30 s to grant stable operating conditions. The exact cycle time for the corresponding experiment is annotated in the figure.

Particle emission monitoring is performed locally via the application of low-cost PM-sensors (spatial PM monitoring) and further down the line at the outlet of the filter house in order to monitor the total emission both with a low-cost PM-sensor and a highly developed laboratory aerosol spectrometer (cf. Sect. 2.2).

The employed test dust was Pural SB[®]. It is a free-flowing test dust with a mass median diameter of approx. $45 \mu\text{m}$. Nonetheless, there are significant amounts of submicron particles within the test dust [23]. Due to its non-agglomerating behavior, the dust tends to cause high emissions in filter tests [24].

2.3 Aerosol Measurement Technology

Emission measurements were performed employing two different types of optical particle counter. On the one hand,

low-cost PM-sensors of the model OPC-N3 by the manufacturer Alphasense were mounted at the blast pipe of each individual filter bag. Each sensor is equipped with a sampling hose in order to measure the emission close to the source at the outlet of the filter bag. Another low-cost PM-sensor was placed at the outlet of the filter house in order to monitor the total dust emission (Fig. 3).

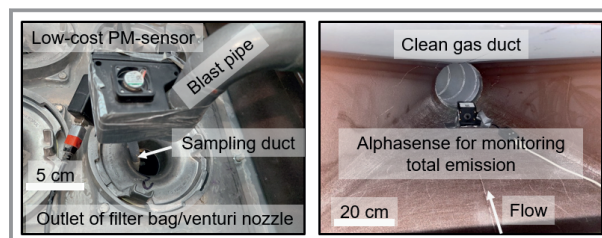


Figure 3. Photograph of the positioning of low-cost PM-sensors at the individual filter bag and for monitoring of the total dust emission on the clean gas side.

As reference, a highly developed laboratory aerosol spectrometer (Promo[®] 2000 with welas[®] 2100 sensor) of the manufacturer Palas[®] was also installed on the clean gas side (cf. Fig. 1). Several key specifications of the two different devices are summarized in Tab. 1.

The low-cost sensors were not calibrated against the reference. The index of refraction of the test dust was not considered in the configuration of the measurement devices (standard setting). The density of the test dust was adjusted in the configuration of the Palas[®] system and via adjustment of the “bin weighting index” of the Alphasense sensor. While the Palas[®] system has an implemented coincidence correction and takes into account border-zone errors, there is no information available whether or not the Alphasense sensor internally corrects potential measurement errors [27].

Table 1. Overview of sensor specifications [25, 26].

Device	OPC-N3	Promo [®] 2000 with Welas [®] 2100
Manufacturer	Alphasense	Palas [®]
Measurements	Mass-based concentration: PM ₁ , PM _{2.5} , PM ₁₀ ; Count rate and size resolved particle counts	Mass and number based total concentration, size distributions, size resolved PM _x conversion
Maximum concentration	2000 $\mu\text{g m}^{-3}$; coincidence probability of 0.84 at 1000 $\# \text{ cm}^{-3}$	500 000 $\# \text{ cm}^{-3}$
Detectable size range	0.35–40 μm	0.2–10 μm ; 0.3–17 μm ; 0.6–40 μm (user selectable)
Size categorization	24 bins	64 bins per decade
Approximate cost (including required cables & connectors)	≈ 400 €	> 30 000 €
Length x Width x Height	75 mm × 45 mm × 63.5 mm	245 mm × 100 mm × 80 mm (Welas [®] sensor only)
Response time	≈ 1 s	≈ 1 s
Volume flow	5.5 L min ⁻¹ ; 280 mL min ⁻¹ (sample)	5 L min ⁻¹
Configuration	$\rho_{\text{particle}} = 2800 \text{ kg m}^{-3}$; $n_{\text{aerosol}} = 1.5$; spherical particles	$\rho_{\text{particle}} = 2800 \text{ kg m}^{-3}$; $n_{\text{aerosol}} = 1.59$; spherical particles

2.4 Filter Media and Methodology for the Detection of Particle Emission Hotspots

Tab. 2 lists the employed filter media. Note that the emission contribution of the filter media plays a subordinate role when compared to the investigated emission hotspots in the different test scenarios.

Filter medium A (scenario 1) is a membrane filter medium (high separation efficiency). Sealing the seams of the filter bag enables test conditions with ideal emission behavior. A filter bag without sealed seams shows increased continuous particle emissions during the initial filtration cycles, as particles can penetrate the seams of the filter bag. For the investigations (Fig. 1), the seams of all but one filter bag were sealed. The filter bag without sealed seams was a factory-new bag for each run and filter position. The bags with sealed seams have not been aged prior to the investigations. Due to the high separation efficiency of the membrane, significant filter aging effects due to agglomeration of particles within the filter matrix are not expected over the course of the experiments.

Filter medium B (scenario 2 & 3) is a typical polyester needle-felt. The filter bags have been aged prior to the investigation (400+ filtration cycles each). Since the experiments in scenario 2 and 3 focus on leak detection, the emission contribution of the intact bags is negligible compared to the strong emission hotspots and further filter aging does not impact the results.

3 Results

The following section presents the experimental results from scenario 1 and scenario 2 (see Fig. 1). Note that scenario 3 can be found in the SI.

3.1 Localization of a Temporal Emission Hotspot (Seams of a Single Filter Bag) – Scenario 1

During the initial filtration cycles of a factory new bag (or filter medium), increased particle penetration is possible, as the deposition of particles within the filter matrix over time increases the separation efficiency. This effect is commonly referred to as filter aging and is accounted for in test procedures for the characterization of filter media [28]. In order to create temporal particle emission hotspots, this behavior was exploited as the seams of all but one filter bag were sealed. The sealed bags enable the ideal emission behavior with defined peaks after each regeneration, whereas the bag with the regular seam is subject to increased particle penetration during the ini-

tial filtration cycles. Fig. 4 shows the temporal and spatial particle emission profile of the measurement where bag number one was the factory-new bag without sealed seams.

The particle emission contribution of the filter bag with open seams dominates the total particle emission. After several cleaning cycles, both the total emission (Palas® – total) and the local emission at the filter bag with regular seams decrease, indicating clogging of the seams. As the pressure for filter regeneration was kept at a moderate level of 3 bar, ideal emission behavior with defined peaks after jet-pulse cleaning and zero emission during the filtration phase is reached and maintained during the experiment.

A summary of the experimental results repeating the procedure for each filter position is shown in Tab. 3 with regards to the average PM concentrations during the experiments. Note that concentrations are subject to fluctuating flow conditions within the baghouse, as larger volume flows occur at the recently regenerated bag [22, 29]. Nonetheless, the values are suitable for a semi-quantitative comparison of different (spatial) emission levels.

Table 2. Specifications of employed filter media

Medium	Area weight [g m ⁻³]	Thickness [mm]	Permeability (200 Pa) [L dm ⁻² min ⁻¹]	Fiber material & remarks
A (membrane)	500	1.9	30	PPS (heat set) with laminated ePTFE membrane
B (needle-felt)	600	2	70	PE, singed upstream side

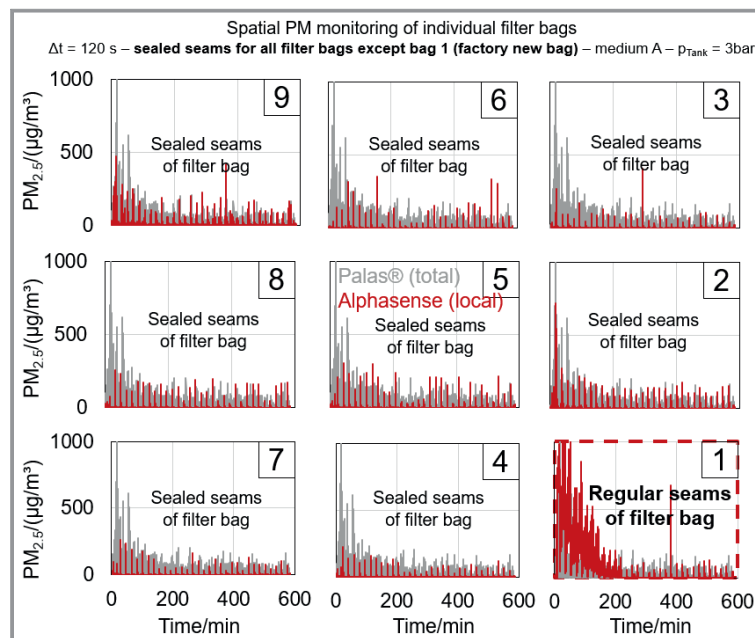


Figure 4. Spatial PM_{2.5} profile with bag 1 as a temporal emission hotspot due to the seams of the filter bag.

Table 3. Summary of measurements regarding the spatial identification of a temporal emission hotspot ($\Delta t = 120$ s, filter medium A, $p_{\text{tank}} = 3$ bar).

Local measurement bag no.		Bag with regular seams ^{a)}									All bags with sealed seams
		9	8	7	6	5	4	3	2	1	
1	Avg. PM _{2.5} [$\mu\text{g m}^{-3}$]	0.3	0.4	0.3	0.5	0.4	0.4	0.3	0.4	72.8	0.3
	Avg. PM ₁₀ [$\mu\text{g m}^{-3}$]	3.7	5.0	3.8	4.3	3.3	4.0	2.2	3.0	860.3	4.0
2	Avg. PM _{2.5} [$\mu\text{g m}^{-3}$]	0.3	0.3	0.3	0.5	0.3	0.3	0.4	82.0	0.8	0.3
	Avg. PM ₁₀ [$\mu\text{g m}^{-3}$]	7.5	7.5	6.2	9.0	5.3	6.5	5.2	416.4	13.0	8.4
3	Avg. PM _{2.5} [$\mu\text{g m}^{-3}$]	1.2	1.7	2.1	0.3	0.3	0.8	121.4	1.2	0.3	1.5
	Avg. PM ₁₀ [$\mu\text{g m}^{-3}$]	10.8	13.3	14.8	3.7	3.4	7.3	815.1	12.0	2.7	11.0
4	Avg. PM _{2.5} [$\mu\text{g m}^{-3}$]	0.3	0.3	0.3	0.4	1.4	149.3	0.2	0.4	0.2	0.3
	Avg. PM ₁₀ [$\mu\text{g m}^{-3}$]	2.2	2.5	2.6	3.4	11.1	1812.9	1.6	3.6	2.6	2.5
5	Avg. PM _{2.5} [$\mu\text{g m}^{-3}$]	0.2	0.4	0.2	1.4	20.9	0.3	0.4	0.4	0.4	0.5
	Avg. PM ₁₀ [$\mu\text{g m}^{-3}$]	1.7	3.7	1.9	13.8	117.2	2.8	3.1	3.2	2.8	5.9
6	Avg. PM _{2.5} [$\mu\text{g m}^{-3}$]	0.2	0.2	0.2	18.1	0.1	0.2	0.5	0.3	0.2	0.2
	Avg. PM ₁₀ [$\mu\text{g m}^{-3}$]	1.5	1.4	1.2	184.3	0.7	1.2	6.9	2.2	3.5	3.2
7	Avg. PM _{2.5} [$\mu\text{g m}^{-3}$]	0.9	0.6	25.1	0.3	0.4	0.5	0.2	0.2	0.3	0.4
	Avg. PM ₁₀ [$\mu\text{g m}^{-3}$]	9.8	9.0	509.2	3.6	3.1	5.3	1.7	1.4	2.0	2.6
8	Avg. PM _{2.5} [$\mu\text{g m}^{-3}$]	0.6	28.2	1.3	0.4	0.4	0.5	0.3	0.3	0.4	0.3
	Avg. PM ₁₀ [$\mu\text{g m}^{-3}$]	6.9	705.4	15.2	3.8	5.0	4.9	2.7	2.5	2.3	5.2
9	Avg. PM _{2.5} [$\mu\text{g m}^{-3}$]	308.3	0.4	0.3	1.4	1.9	2.7	1.3	0.9	0.7	0.4
	Avg. PM ₁₀ [$\mu\text{g m}^{-3}$]	8530.0	9.0	4.4	24.9	40.5	62.9	23.1	13.7	10.3	6.4
Total emission (Palas®)	Avg. PM _{2.5} [$\mu\text{g m}^{-3}$]	78.0	49.9	24.8	21.9	n.a.	9.0	10.6	12.9	5.9	1.4
	Avg. PM ₁₀ [$\mu\text{g m}^{-3}$]	1055.1	688.3	313.6	281.4	n. a.	127.5	133.4	162.4	75.5	16.8

a) all other bags with sealed seams.

The single bag with regular seams can be easily identified due to the increased PM concentrations at each position (compare the diagonal of the table). The average PM concentrations are subject to long averaging intervals (30 filtration cycles for each bag with $\Delta t = 2$ min), where the highest emissions occur during the initial cycles, where constant particle penetration through the seams is possible. Therefore, the absolute concentration peaks and the concentrations during these corresponding cycles are significantly higher compared to the average of the total experimental duration displayed in Tab. 3. At all other measurement positions with bags with sealed seams, the resulting PM concentrations are lower and almost at a zero level. The concentrations are similar to the concentrations obtained during a previous reference measurement, where all bags had sealed seams and correspond to ideal emission behavior (right column of the diagram).

An exception is bag number nine, where consistently higher concentrations are detected compared to the other bags. This is also in agreement with the measurement where bag 9 was exchanged with a factory-new bag with regular seams, as

the measured concentrations exceed the concentrations from the other positions by a large margin. Nonetheless, the concentrations at bag 9 remain lower than the concentrations of the respective bag with regular seams. A concise explanation for this outlier is difficult, as a direct comparison between the total and local concentrations is not possible and it remains unclear if the emission were indeed higher at this measurement position, e.g., due to faulty installation of the bag. Another possibility is a systematic error of the sensor itself, however sensor 9 did not show notable differences during the reference measurement (all bags with sealed seam) and in consecutive measurement campaigns.

There is no direct correlation between the total concentration measured by the Palas® reference and the average concentrations measured by the low-cost sensors. Thus, an estimation of the intensity of the total PM emission from the local measurement is not possible and the sensor may merely serve as a qualitative monitoring tool. However, the spatial identification of the temporal emission source was very reliable for each measurement position.

Another experiment can be found in the SI, where an entire row of filter bags (position 4, 5 and 6) was exchanged with factory new bags. The corresponding row could also be reliably identified as the main contribution to the total emission with the help of low-cost PM-sensors.

3.2.1 Localization of a Strong Continuous Emission Hotspot (Leak in a Single Filter Bag) – Scenario 2

While the seams of the filter bag mainly serve as a temporal origin for dust emissions during the initial filtration cycles, their impact on the total dust emission is comparably small when related to the total lifetime of the filter bag. Leaks may cause sudden significant increase in dust emissions and are one of the major reasons for the shutdown of filter houses.

In scenario 2, the filter bag at position made from filter medium B was pierced with a cannula of 3 mm diameter in order to create an increasing number of leaks over multiple experimental runs ($\Delta t = 30$ s). Fig. 5 displays the spatial PM_{2.5} emission profile for the initial experiment (one leak).

Similar to the experiments shown in Sect. 3.1, the position of the damaged filter bag can be easily identified from the measured PM data. The constant particle flux through the leak is indicated via the total concentration measured by the Palas® reference in the background of Fig. 5. The surrounding filter bags mostly show the ideal emission behavior, where distinct emission peaks are detected after jet-pulse cleaning. A preceding measurement before creating the leaks can be found in the SI and also shows the ideal emission behavior for all measurement positions.

When increasing the number of leaks, the bypass flow penetrating to the clean gas side without filtration also increases, resulting in higher clean gas concentrations. When comparing the measurements with one leak and six leaks regarding the PM concentrations at the damaged filter bag, a measurement error of the low-cost PM-sensor can be observed (Fig. 6). The same error likely occurs during minute 100–150 of the experiment with one leak.

Even though the leak area increases, the measured PM_{2.5} concentration of the low-cost sensor at the emission hotspot decreases, seemingly giving an indication of a zero-emission level. The PM₁₀ concentration shows the actual correct trend of increasing concentration with increasing leak area/bypass flow. This correlation (high PM₁₀ and low PM_{2.5} at high concentration conditions and no change in raw gas particle size distribution) is a clear indication for a coincidence error, where multiple particles pass the measure-

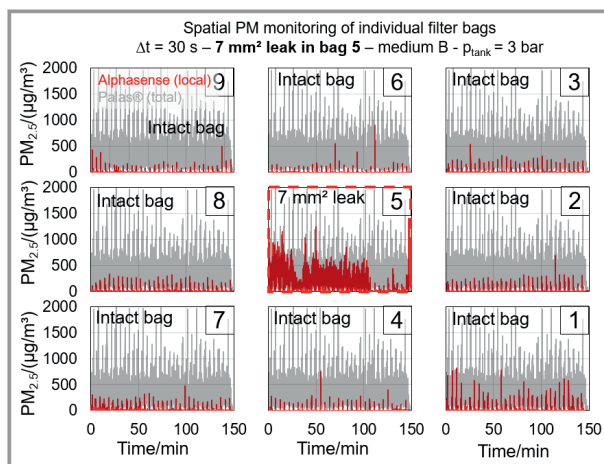


Figure 5. Spatial PM_{2.5} profile with bag 5 as a strong continuous emission hotspot due a leak of 3 mm diameter.

ment volume of the low-cost PM-sensor simultaneously. A more in-depth explanation of the coincidence error, referencing the relevant standards, can be, e.g., found in the book by Gail and Gommel [30]. When a particle passes the measurement volume of an optical particle counter, light is scattered at the single particle. The scattered light causes a signal peak at the detector of the sensor. Based on the peak height, particles are classified into the respective optical size class. The number of counting events in a certain time duration related to the measurement volume yields the particle number concentration. The determined particle size, particle density, shape factor and index of refraction, enable the calculation of particle mass concentrations from the previously determined particle number concentration. Based on their size, they contribute to the corresponding mass-based PM concentrations (e.g., PM_{2.5} or PM₁₀). When multiple

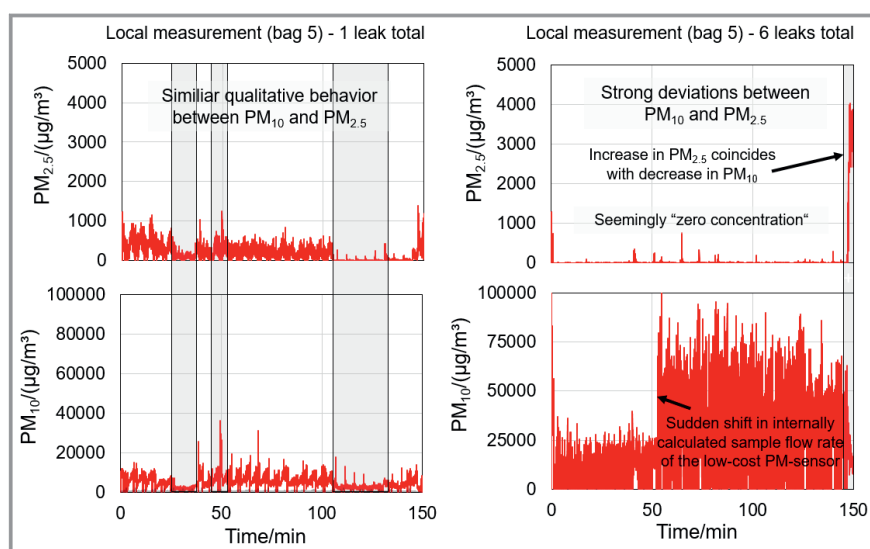


Figure 6. Comparison of the measured local dust emissions for one and six leaks regarding PM_{2.5} and PM₁₀ concentrations.

particles pass the measurement volume simultaneously, the signal peak is overestimated, and the individual counting events cannot be distinguished. Thus, the number of counting events is lower, but the determined particle size is higher than in reality [27, 30–32]. If this wrongly allocated diameter exceeds the $PM_{2.5}$ size class and is instead classified as a PM_{10} relevant particle, the $PM_{2.5}$ concentration decreases while the PM_{10} concentration further increases. The decrease of detected particles in the smaller size fraction can also be derived from the particle size distribution (cf. Fig. 9). In general, coincidence-free measurement is limited by a maximum count-rate that depends, e.g., on the size of the measurement volume. Highly developed aerosol spectrometers (or optical particle counters) may employ a coincidence correction, as is the case for the Palas® reference [25]. It is unknown, whether or not the employed low-cost sensor utilizes similar methods.

At the end of the experiment and the end of dust dosage (no emission bypass through the leak), the PM_{10} concentration decreases, which is linked to an increase in $PM_{2.5}$ concentration. The number of particles passing the measurement volume decreases, so that the impact of the coincidence error is lower and counting events can be correctly distinguished and particles are allocated to the correct $PM_{2.5}$ relevant size classes.

The measurement error puts the quantitative accuracy of the low-cost sensor into question, however qualitative or semi-quantitative information regarding the size of the leak and its position may still be gained. Fig. 7 shows the spatial PM_{10} profile for the case of six leaks total, as the $PM_{2.5}$ reading of the sensor is greatly affected by coincidence effects.

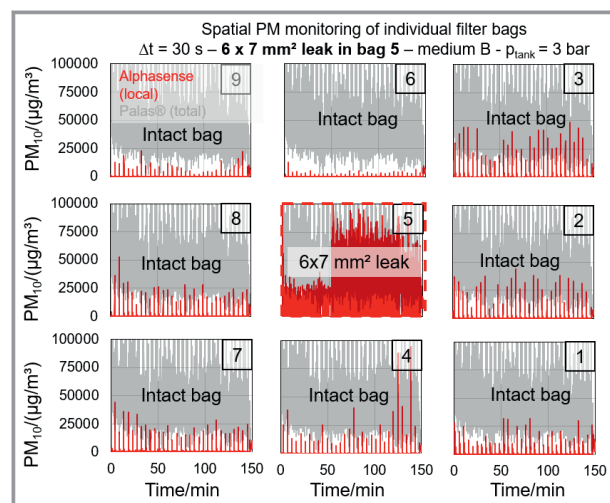


Figure 7. Spatial PM_{10} profile with bag 5 as a strong continuous emission hotspot due to six leaks of 3 mm diameter each.

The dust emission has increased considerably (average of $2000 \mu\text{g m}^{-3} PM_{2.5}$ and $40\,000 \mu\text{g m}^{-3} PM_{10}$ – cf. Palas® reference in Fig. 6), greatly exceeding the manufacturer specifications of the sensor (see Tab. 1). However, even for this

case, a clear identification of the damaged bag is possible and all other low-cost PM-sensors show the expected ideal behavior. The sharp increase of the particle concentration at about 50 min time at position 5 is caused by a sudden shift in the internally determined sensor flow rate. A decrease in flow rate causes higher concentrations, as the counting events are related to a smaller volume for the determination of particle number concentration and the respective PM values. A more in-depth discussion of this measurement artifact (sample flow rate) can be found in the SI. The findings further demonstrate the limitations of the sensors, which are not suitable for accurate concentration readings under these conditions.

Despite the resident measurement artifacts, a reliable identification of the strong emission hotspot could be achieved by operating a network of low-cost PM-sensors within the baghouse filter. There is a clear potential for improved process monitoring applying low-cost PM-sensors as a cheap monitoring tool in order to identify the origin of dust emissions and qualitative trends regarding the emission level. The investigations in scenario 3 in the appendix show that measurement close to the hotspot is crucial for a successful identification. The leak in the plenum plate could not be allocated via the sensor data from the positions at the individual filter bags. Nonetheless, the low-cost PM-sensor monitoring the total dust emission correctly detected the concentration increase, offering an indication on the required maintenance and showing that the filter bags are intact and not the origin of the increased emission.

3.2.2 Impact of Leak Diameter on the Detection Capabilities of the Low-Cost PM Sensors – Scenario 2

While the position of the leak at bag number 5 could be reliably identified, coincidence effects were observed in the form of an increasing PM_{10} concentration and a decreasing $PM_{2.5}$ concentration at the PM emission hotspot. Presumably, multiple particles pass the measurement volume simultaneously under high concentration conditions, causing the detection of a lower particle number concentration with a larger overall particle size as the individual counting events can no longer be distinguished. Fig. 8 shows the average concentrations of the total dust emission as determined by the Palas® reference and the low-cost sensor further down the clean gas duct (Fig. 3), as well as the local concentration measured by the low-cost PM-sensor positioned at the emission hotspot (bag 5).

The Palas® reference shows the correct behavior reported in literature, whereby the dust concentration increases linearly with leak area [16, 17]. The deviation to perfect linear behavior (especially visible for the change from four to six leaks total) originates from smaller fluctuations regarding the dust dosage and the possibility of particle deposition and bridging of the leaks during the experiment (see Fig. 1 where part of the circular 3 mm leak is blocked by particles).

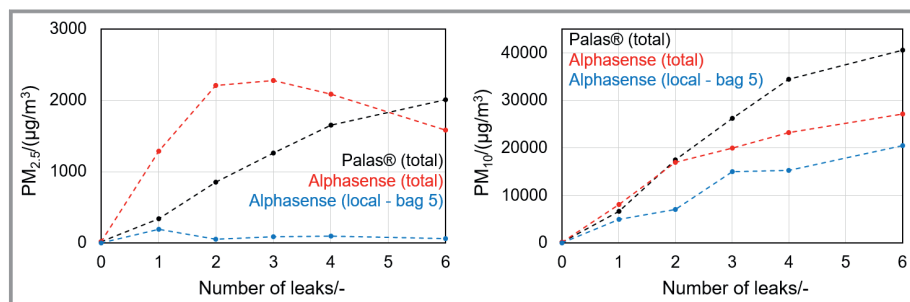


Figure 8. Optically determined average PM clean gas concentration dependent on the number of leaks (3 mm diameter each).

The average number concentration detected by the Palas® reference during the experiment with six leaks was approx. 4000 cm^{-3} (maximum peak at approx. $25\,000 \text{ # cm}^{-3}$) so that a coincidence error of the reference is unlikely [25].

The Alphasense sensor also measuring the total concentration in the clean gas duct shows a linear increase for the first two leaks. Afterwards, the slope of the average PM₁₀ concentration curve decreases. The effect on PM_{2.5} concentration is more pronounced by the larger amount of particles penetrating to the clean gas side. Adding a third leak results in a seemingly constant PM_{2.5} concentration and adding even further leaks causes the discussed drop in PM_{2.5} concentration that is linked to the coincidence error.

The locally determined concentrations (blue curve) also show the previously discussed coincidence effect. While there is an increase in PM_{2.5} concentration from none to one leak, the PM_{2.5} concentration does not increase further and an increase in concentration is only notable via the increase of detected PM₁₀ relevant particles.

The particle size distributions of the total dust emission (Fig. 9) further confirm the measurement error. For the case of zero leaks, the size distributions are in relatively good agreement. With increasing number of leaks, the amount of particles classified in the smaller size classes decreases for the low-cost PM-sensor (see, e.g., drop in the smallest size

class). The number of counting events of bigger particles increases respectively (e.g., increase of $10 \mu\text{m}$ particles). The correct trend of a uniform increase of counting events across all size classes is monitored by the Palas® reference.

Even though the measurements of the low-cost PM-sensors are strongly affected by the coincidence error, semi quantitative information regarding leak size

can be gained. A decrease in PM_{2.5} readings linked to an increase in PM₁₀ concentrations is an indication for high particle concentrations, exceeding the maximum counting rate. While the low-cost PM-sensor did not correctly measure the linear increase of clean gas concentration with increase in leak diameter, a further increase in PM₁₀ concentrations was recorded so that the overall emission level caused by the different numbers of leaks can be distinguished.

4 Summary and Outlook

Experiments regarding the identification of spatial particle emission hotspots were performed in a small-scale bag-house filter by operating a network of low-cost PM-sensors for emission monitoring of each individual filter bag. The experiments were divided into three scenarios.

In the first scenario, one of the nine filter bags made from a membrane filter medium with sealed seams was exchanged with a factory-new bag with regular seams. As the seams enable particle penetration during the initial filtration cycles before clogging, the exchanged filter bag serves as a temporal emission hotspot. Increased concentrations were measured by the low-cost PM-sensor positioned at the

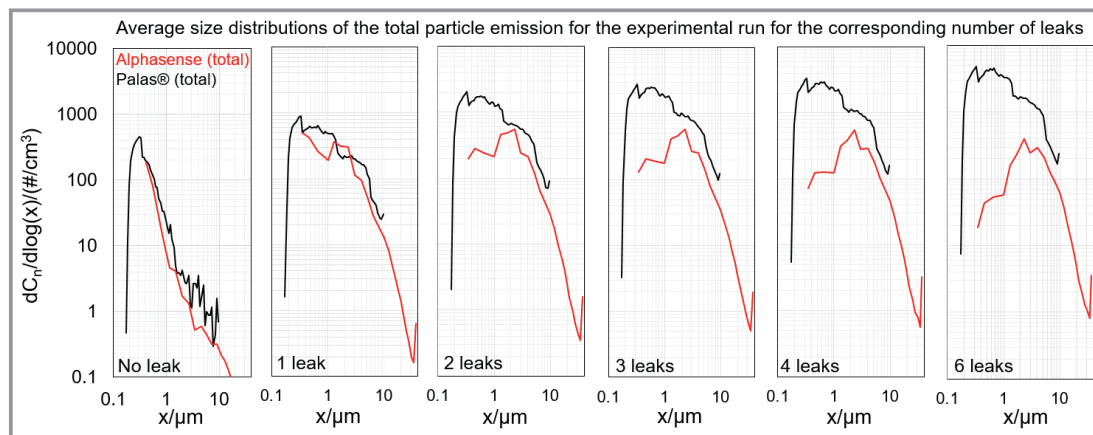


Figure 9. Comparison of particle size distributions of the total particle emission dependent on the number of leaks for the low-cost PM-sensor and the reference.

emission hotspot for each measurement run. The concentrations measured at all other bags followed an ideal behavior where a distinct particle emission peak is detected for a short duration after filter regeneration. The investigations demonstrate the possibility of spatial identification of an emission hotspot by implementing a network of low-cost PM-sensors.

In the second scenario, an increasing number of defined leaks (3 mm diameter each) were introduced in a single filter bag made from a standard needle-felt. The spatial identification of the damaged bag was possible for each case, however, increased concentrations due to higher numbers of leaks/a higher leak area led to coincidence errors for the low-cost PM-sensor. Here, the number of counting events in the PM_{2.5} relevant size classes was very small, as multiple smaller particles passing the measurement volume of the sensor simultaneously were presumably detected as fewer and larger particles, where the detected particle size exceeded the PM_{2.5} fraction and was only accounted for in the PM₁₀ relevant size fractions. Even though the measurements of the low-cost PM-sensors are heavily influenced by the coincidence error, an increasing PM₁₀ concentration was detected with increasing numbers of leaks, enabling the estimation of leak size. The concentrations detected by low-cost PM-sensors have to be evaluated carefully and both, PM_{2.5} and PM₁₀ signals have to be considered in order to give accurate interpretations on the current particle emission level (especially in the case of higher concentration regions where coincidence errors become relevant).

In the third and final scenario, a leak was introduced into the plenum plate of the filter house without direct monitoring of the emission source. The sensors positioned at the filter bag measured an ideal emission behavior. The increase of the particle emission was only detected by sensors monitoring the total dust emission. Thus, positioning close to the source is important when employing low-cost PM-sensors for emission monitoring.

The experiments in the small-scale baghouse filter showed the possibilities of reliable identification of leaks as well as the potential for the estimation of leak sizes when correctly interpreting sensor data. Coincidence errors for higher particle concentrations and quantitative deviations to state-of-the-art optical particle counters limit the quantitative accuracy and reliability of the sensors. Further technical limitations are long term stability and the use of the sensors in demanding filtration applications (corrosive gases, higher temperatures). Nonetheless, leak detection poses one of the most prominent potential applications when implementing low-cost PM-sensors in technical facilities for (spatial) PM monitoring. Suitable sensors could greatly improve process monitoring of filter houses and the operation and maintenance procedures by identifying damaged filter elements.

Supporting Information

Supporting Information for this article can be found under DOI: <https://doi.org/10.1002/cite.202200116>.

We acknowledge the financial support and close cooperation of Filterkonsortium at KIT. Filterkonsortium at KIT unites leading companies in the fields of fiber and media production, assembly, plant engineering and measurement technology with the research activities of the research group Gas-Particle-Systems of the Institute of Mechanical Process Engineering and Mechanics (MVM). The members of Filterkonsortium at KIT are as follows: BWF Tec GmbH & Co. KG, ESTA Apparatebau GmbH & Co. KG, Evonik Fibres GmbH, Freudenberg Filtration Technologies SE & Co. KG, Junker-Filter GmbH, MANN+HUMMEL GmbH, PALAS GmbH, Sick AG.

We acknowledge the collaboration of Enes Malik Akdas and Daniel Arnaud Sokoundjou Fotsing for their help in conducting the experiments.

We acknowledge that part of the materials (Sect. 3.1) have been first presented in FiltCon 2021 conference, USA organized by the American Filtration and Separations Society. Parts of this work were presented at FILTECH 2022. Open access funding enabled and organized by Projekt DEAL.

Symbols used

C_n	[# cm ⁻³]	particle number concentration
n_{aerosol}	[-]	index of refraction
r_{particle}	[kg m ⁻³]	particle density
x	[μm]	particle diameter

Abbreviations

PM	particulate matter
PM _x	weighted mass based particulate matter concentration whereby the x refers to the corresponding size fraction

References

- [1] H. J. Imminger, P. Krug, *Cleanable filter media go close to zero emission*, Filtech, Cologne, October 2019.
- [2] F. Löffler, *Staubabscheiden*, Georg Thieme, Stuttgart 1988.
- [3] E. Schmidt, *Fortschr.-Ber. VDI-Z.* 1998, Reihe 3, Nr. 546.
- [4] J. Binnig, J. Meyer, G. Kasper, *Powder Technol.* 2009, 189 (1), 108–114. DOI: <https://doi.org/10.1016/j.powtec.2008.06.012>
- [5] D. Leith, M. J. Ellenbecker, *Aerosol Sci. Technol.* 1982, 1 (4), 401–408. DOI: <https://doi.org/10.1080/02786828208958604>

- [6] P. Bächler, V. Löschner, J. Meyer, A. Dittler, *Process. Saf. Environ. Prot.* **2022**, *160*, 411–423. DOI: <https://doi.org/10.1016/j.psep.2022.02.005>
- [7] VDI 3677 Blatt 1, *Filtering Separators – Surface Filters*, Beuth Verlag, Berlin **2010**.
- [8] P. Spanring, N. A. Nowak, T. Laminger, G. Mauschwitz, *Investigation of regeneration stability of pulse-jet regenerated filter media under laboratory test conditions*, Filtec, Cologne, October **2019**.
- [9] H. Leubner, U. Riebel, *Chem. Ing. Tech.* **2003**, *75* (12), 82–86. DOI: <https://doi.org/10.1002/cite.200390027>
- [10] S. Schiller, H. J. Schmid, *Powder Technol.* **2015**, *279*, 96–105. DOI: <https://doi.org/10.1016/j.powtec.2015.03.048>
- [11] H. Leubner, *Die simultane Abscheidung von Stäuben und sauren Gasen (HCl, SO₂) aus Abgasströmen durch Precoatfiltration bei 150–300°C*, Ph. D. Thesis, BTU Cottbus-Senftenberg **2004**.
- [12] N. Khirouni, A. Charvet, D. Thomas, D. Bémer, *Process. Saf. Environ. Prot.* **2020**, *138*, 1–8. DOI: <https://doi.org/10.1016/j.psep.2020.02.040>
- [13] G. Mouret, D. Thomas, S. Chazelet, J. C. Appert-Collin, D. Bémer, *J. Aerosol. Sci.* **2009**, *40* (9), 762–775. DOI: <https://doi.org/10.1016/j.jaerosci.2009.04.010>
- [14] C. R. de Lacerda, P. Bächler, A. D. Schwarz, R. Sartim, M. L. Aguiar, A. Dittler, Impact of Seams on the Operating Behavior of Surface Filters Regarding Particle Emissions, *Chem. Eng. Technol.* **2022**, *45* (7), 1354–1362. DOI: <https://doi.org/10.1002/ceat.202200132>
- [15] J. Li, Q. Wu, Y. Huang, Z. Sun, J. Li, D. Wu, *Process Saf. Environ. Prot.* **2022**, *158*, 282–290. DOI: <https://doi.org/10.1016/j.psep.2021.12.012>
- [16] B. Bach, E. Schmidt, *J. Hazard. Mater.* **2007**, *143* (3), 673–676. DOI: <https://doi.org/10.1016/j.jhazmat.2007.01.093>
- [17] O. Kurtz, J. Meyer, G. Kasper, *Particuology* **2017**, *30*, 40–52. DOI: <https://doi.org/10.1016/j.partic.2016.08.001>
- [18] O. Kurtz, *Ursachen für Emissionen in Mehrfilteranlagen*, Ph. D. Thesis, Karlsruhe Institute of Technology **2017**.
- [19] G. Wiegler, *Gasmestechnik in Theorie und Praxis*, Springer Vieweg, Wiesbaden **2016**. DOI: <https://doi.org/10.1007/978-3-658-10687-4>
- [20] J. Li, X. Lu, W. F. Wang, *Opt. Fiber Technol.* **2020**, *57*, 102218. DOI: <https://doi.org/10.1016/j.yofte.2020.102218>
- [21] P. Bächler, J. Meyer, A. Dittler, *Gefahrst. Reinhalt. Luft.* **2019**, *79* (11–12), 443–450. DOI: <https://doi.org/10.37544/0949-8036-2019-11-12-49>
- [22] P. Bächler, J. Szabadi, J. Meyer, A. Dittler, *J. Aerosol. Sci.* **2020**, *150*, 105644. DOI: <https://doi.org/10.1016/j.jaerosci.2020.105644>
- [23] P. Bächler, J. Meyer, A. Dittler, *Aerosol Sci. Technol.* **2022**, *56* (4), 394–402. DOI: <https://doi.org/10.1080/02786826.2022.2027335>
- [24] S. Sobich, J. Meyer, A. Dittler, G. Kasper, *Baghouse filtration: a praxis relevant media parameter to determine an emissions level of a pulse-jet cleanable filter*, Filtec, Cologne, March **2018**.
- [25] www.palass.de/product/aerosolsensorwelas2100 (Accessed on May 13, 2022)
- [26] www.alphasense.com/wp-content/uploads/2019/03/OPC-N3.pdf (Accessed on May 13, 2022)
- [27] L. Mölter, *Bestimmung der Anzahlverteilung von Tracerpartikeln*, Fachtagung Lasermethoden in der Strömungsmesstechnik, Braunschweig, September **2006**.
- [28] DIN ISO 11057, *Air quality – Test method for filtration characterization of cleanable filter media*, Beuth Verlag, Berlin **2011**.
- [29] X. Simon, D. Bémer, S. Chazelet, D. Thomas, R. Régnoer, *Powder Technol.* **2010**, *201* (1), 37–48. DOI: <https://doi.org/10.1016/j.powtec.2010.02.036>
- [30] L. Gail, U. Gommel, *Reinraumtechnik*, Springer Vieweg, Wiesbaden **2018**. DOI: <https://doi.org/10.1007/978-3-662-54915-5>
- [31] J. Raasch, H. Umhauer, *Fortschr.-Ber. VDI-Z.* **1984**, Reihe 3, Nr. 95.
- [32] B. Sachweg, H. Umhauer, F. Ebert, H. Büttner, R. Friehmelt, *J. Aerosol. Sci.* **1998**, *29* (9), 1075–1086. DOI: [https://doi.org/10.1016/S0021-8502\(98\)80004-9](https://doi.org/10.1016/S0021-8502(98)80004-9)

DOI: 10.1002/cite.202200116

Spatially Resolved Online Leak Detection in a Baghouse Filter Applying Low-Cost PM-Sensors

Peter Bächler, Jörg Meyer, Achim Dittler*

Research Article: The identification of leaks in baghouse filters is a great challenge, as even small leaks (several ppm of installed filter area) can contribute greatly to the total dust emission so that emission limits are exceeded. The article demonstrates the potential application of cheap distributed particle sensors for spatial online leak detection and improved process monitoring.



Supporting Information
available online

